Enabling portable multiple-line refreshable Braille displays with electroactive elastomers

Gabriele Frediani[a], James Busfield[b], Federico Carpi [a,*]

[a] *University of Florence, Department of Industrial Engineering, Via di S. Marta, 3 - 50139 Florence, Italy.*

[b] *Queen Mary University of London, School of Engineering & Materials Science, Mile End Road, E14NS, London, UK.*

Abstract

Full-page (multiple-lines), electrically refreshable, portable and affordable Braille displays do not currently exist. There is a need for such an assistive technology, which could be used as the Braille-coded tactile analogue for blind people of the digital tablets used by sighted people. Turning those highly desirable systems into reality requires a radically new technology for Braille dot actuation. Here, we describe standard-sized refreshable Braille dots based on an innovative actuation technology that uses electro-responsive smart materials known as dielectric elastomers. Owing to a significantly reduced lateral size with respect to conventional Braille dot drives, the proposed solution is suitable to array multiple dots in multiple lines, so as to form full-page Braille displays. Furthermore, a significant reduction also of the vertical size makes the design suitable for the development of thin and lightweight displays, thus enabling portability. We present the first prototype samples of these new refreshable Braille dots, showing that the achievable active displacements are adequately close to the standard Braille requirements, although the force has to be further improved. The paper discusses the remaining challenges and describes promising strategies to address them.

Keywords: actuator; braille; blind; dielectric elastomer; display; electroactive; multiple line; polymer; portable; refreshable; tactile.

---

[*] Corresponding author. Tel.: +39 055 2758660;
E-mail address: federico.carpi@unifi.it.

1. Introduction

The world's roughly 314 million blind and visually impaired people are largely excluded from today's digital revolution in information and communication technologies. Indeed, displays of computers, portable devices, touch screens and so forth are conceived to bring text and images via the sense of sight.

Visually impaired people can access digital information only via text-to-speech readers. However, conveying information using sound is not always effective. Indeed, the interpretation of text based only on listening might be limited, for example, by the impossibility of a continuous backtrack. Furthermore, the presence of other people nearby might require the use of headphones to protect privacy or not to disturb, whilst a noisy environment might provide an additional challenge.

Overcoming these problems requires refreshable Braille displays. They are conceived as electronically controllable tactile interfaces allowing blind users to read text presented in the Braille code via dots that are dynamically raised and lowered. In particular, full-page displays would allow blind people to access via the sense of touch large amounts of structured and dynamic information, like sighted people commonly do via the sense of sight, for example when using computer monitor displays, tablets and smartphones. In other words, full-page displays are needed as the Braille-coded tactile analogue for the blind people of the displays used by the sighted people to visualise text and images.

Commercially available refreshable Braille displays are based on piezoelectric reeds that actuate the Braille dots. The reeds are mounted as a stair stepped stack of cantilevers, each with a Braille pin resting on its free end [1]. This solution limits the whole display to a maximum of two lines of Braille characters [2], which makes backtracking impossible while reading a full page of text. To overcome this limitation, attempts to develop full-page Braille readers based on different types of piezoelectric actuators are in progress, although the only available system developed so far is non-portable and has an estimated cost of about € 60,000 [3].

So, affordable, portable and multiple-line (full-page) Braille displays are needed, as they merely represent technological fiction today. They are required to facilitate access to digital information, as well as to help to improve the Braille literacy rate across the blind population, also with the aim of reducing its high unemployment rate [4].

A paradigm shift from technological fiction to reality requires the ground-breaking creation of a radically new technology for Braille dot actuation. To this end, several alternatives to piezoelectric actuators have been studied. For instance, pneumatically actuated Braille dots with microvalves have been proposed [5], although the need for air pumping and individual dot control limits the portability of the resulting systems. Shape memory alloys have also been investigated as a method of providing actuation, although they show limitations in terms of size, speed and power consumption [6]. Linear actuators vertically pushing Braille dots have been prototyped using either rolled sheets of electrostrictive polymers [7] or tubes of dielectric elastomers [8], although the length of the actuators enlarges the size of the device.

Dielectric elastomer (DE) actuators [9-11] represent the electromechanical transduction technology used in this work too. They belong to the bigger family of electromechanically active polymers [12], which includes a diversity of smart materials studied for various biomedical applications [13]. The most basic configuration of a DE actuator consists of a thin elastomeric layer coated with two compliant electrodes, so as to obtain a deformable capacitor. A voltage V applied between the electrodes results in the following effective electrostatic pressure p on the elastomer surface:

$$p = \epsilon_r \epsilon_0 \left(\frac{V}{d}\right)^2 \qquad (1)$$

where ϵ_0 is the dielectric permittivity of vacuum, ϵ_r is the elastomer's relative dielectric constant and d is the dielectric layer's thickness. This pressure causes a squeezing in thickness and a concurrent surface expansion [11].

The DE actuation technology in general offers attractive properties in terms of large strains, fast, stable and silent operation, compact size, low weight, shock tolerance, low power consumption and no overheating [9-11, 14]. DE actuators show significant potential to develop compact, fast, lightweight and silent electromechanical transducers for tactile interfaces [14]. Studied configurations include cylinders [7, 8, 15], diaphragms [16], buckling membranes [17, 18], planar multi-layer stacks [19] and bistable diaphragms [20]. Nevertheless, so far, none of these proposed configurations seems to be readily applicable to obtain commercially viable Braille displays. This is due to a number of challenges (specific to each approach), related to one or more of the following drawbacks: low forces, low displacements, low response speed, high cell thickness and overall encumbrance, high energy consumption, overheating, manufacturing complexity, short lifetime, low reliability (see details in the previously mentioned references).

Aimed at overcoming the limitations of these state-of-the-art approaches, this paper presents real-size refreshable Braille dots based on DE actuation. The design, working principle, fabrication and a preliminary electromechanical characterization are described in the next sections, following a reminder of the main technical requirements.

2. Technical specifications

The requirements in terms of dimensions and force for a standard Braille dot [1] are presented in Table 1.

Table 1

Specifications of Braille dot parameters for refreshable Braille displays [1].

Dot parameter	**Typical value**
Base diameter	1.5 mm
Height (assuming no force from user's finger)	0.7 mm
Blocking force (dot raised within 0.1 mm of maximum height)	50 mN
Blocking force (dot raised 0.25 mm above reading surface)	150 mN

According to these requirements, the raised Braille dot consists of a quasi-hemispherical cap.

Moreover, besides these geometrical and performance requirements, the dots' actuation technology should comply with electrical safety issues and allow for ease of miniaturization at low production costs, so as to enable compact and cost-effective systems.

Aimed at addressing such needs, this paper presents the concept and a prototype implementation of a radically new kind of Braille dots with intrinsic dynamic actuation.

3. Proposed concept and principle of operation

The concept is based on the particular type of DE technology known as 'hydrostatically coupled' DE (HC-DE) actuation [21]. HC-DE actuators in general are based on an incompressible fluid that mechanically couples a DE-based active part to a passive part interfaced to the load, so as to enable hydrostatic transmission. This general concept was used in this work to conceive a dynamic Braille dot as a bubble-like HC-DE actuator. The device is such that the actuator itself coincides with the dynamic Braille dot. The structure is shown in Fig. 1.

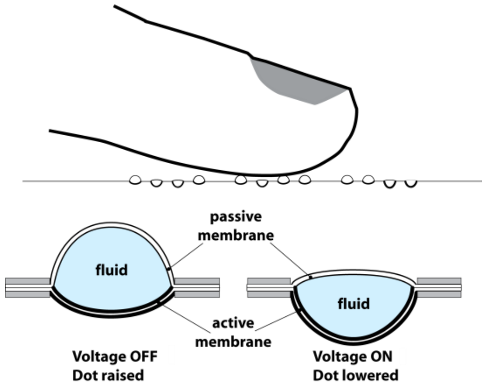

Fig. 1. Schematic drawing of the proposed concept. In order to obtain an array of electrically controllable compact Braille dots (top panel), each dot consists of a bubble-like HC-DE actuator (bottom panel). A lateral section of the actuator/dot is shown in the rest state (bottom, left) and in an electrically induced state due to an applied voltage (bottom, right).

It includes the following parts: an electromechanically active membrane, made of a DE film coated with compliant electrodes; an electromechanically passive membrane, working as the end effector in contact with the finger (either directly, or via any interposed medium); an incompressible fluid contained in a chamber constrained by the two membranes. Both membranes are radially constrained by bonding them to a frame, in the region external to the chamber. The internal fluid is pressurised during manufacturing, so as to provide each membrane with the shape of a roughly spherical cap. The pressurised top membrane works as the Braille cell dot (passive interface with the user's fingertip). The pressurised bottom membrane behaves as a buckling DE actuator. The latter buckles outwards as a voltage difference is applied between its electrodes, while the passive membrane relaxes (as the pressure is reduced) and passively moves inwards, according to the fluid-enabled hydrostatic transmission (Fig. 1). Therefore, the dot is lowered or raised as a voltage is applied or removed, respectively. This principle allows for an electrically safe transmission of actuation from the active membrane to the finger, without any direct contact between them.

This basic structure can be replicated to implement a standard 8-dots Braille cell, as shown in Fig. 2.

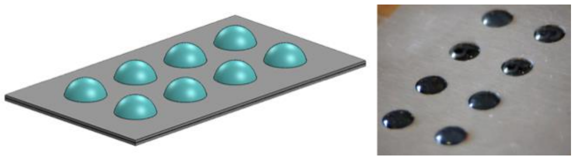

Fig. 2. Array of eight Braille dots based on the proposed configuration, to obtain a dynamic Braille cell: concept (left) and assembled prototype (right).

Prototype dots were manufactured and tested as described in the next sections.

4. Materials and methods

4.1 Manufacturing

The fabrication process consisted of several steps, which are presented in Fig. 3 and are described below.

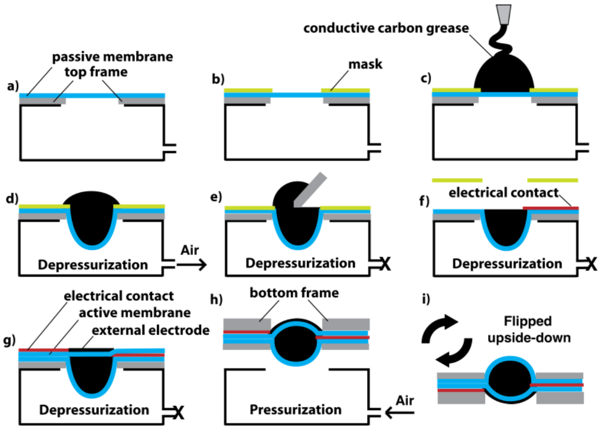

Fig. 3. Braille dot fabrication steps. A dielectric elastomer membrane previously bonded to a PMMA frame is placed over an empty chamber containing a circular hole (a); the membrane is masked, such that the central circular portion, corresponding to the chamber's hole, is left exposed (b); the membrane is coated with conductive carbon grease (c); a depressurization is applied inside the chamber in order to deform the membrane (d); the excess grease is removed (e); the mask is peeled off and the internal electrical contact is applied (f); a second dielectric elastomer membrane is arranged above, a thin layer of carbon grease is deposited on top of it and an electrical contact is created (g); a second circular frame is applied above and the chamber is brought back to atmospheric pressure to release the overstress applied to the passive membrane and detach the obtained structure from the chamber (h); the structure is flipped upside down to be used as a Braille dot (i).

The actuator was assembled using membranes made of commercially available acrylic elastomer films (VHB tape series, by 3M). In particular, four combinations of different grades were tested, as detailed in the next section.

Each membrane was bi-axially pre-stretched by four times, which means that it was subjected to a biaxial pre-strain of 300%. The application of this pre-strain was justified as a consequence of the well-known beneficial effect that consists in an increase in the electromechanical transduction performance, as first documented by Pelrine et al. [11] and later on explained in different ways by Brochu and Pei [9] and Koh et al. [22].

The pre-stretched membrane that had to work as the passive membrane was coupled to a thin metallic support frame, exploiting the fact that their bonding was ensured by the adhesive properties of the membrane's constitutive material. This membrane and its support were then placed over a vacuum chamber (Fig. 3a). An annular mask was applied to the membrane, in order to leave its central circular portion, corresponding to the chamber's hole, exposed (Fig. 3b). To this end the paper liner that came with the VHB tape was used, so as to facilitate the mask removal afterwards. Then, the membrane was coated with a carbon conductive grease (846, M.G. Chemicals, Canada) (Fig. 3c), which was used both as the hydrostatic coupling fluid and the internal electrode for the active membrane; the volume of deposited grease was intentionally in excess, in order to simplify the subsequent steps of the process and ensure adequate filling of the bubble cavity to be created. Afterwards, the chamber was depressurised in order to deform the membrane, so as to obtain a cavity filled in by the grease (Fig. 3d). This procedure avoided that any air bubble remained trapped at the membrane/grease interface, as it would likely be the case if the grease were applied after the creation of the cavity. Subsequently, the excess grease was removed (Fig. 3e), the mask was peeled off and a thin aluminium strip was applied to serve as the internal electrical contact (Fig. 3f). The structure was covered with the prestretched membrane that had to work as the active membrane (again exploiting its inherent adhesive properties), which was then coated with the same type of carbon conductive grease to create the external electrode; then, an aluminium strip was applied to create the external electrical contact (Fig. 3g). A second PMMA frame was finally coupled to the active membrane and the so-obtained actuator was removed from the vacuum chamber by pressurising it (Fig. 3h,i).

The resulting shape of the stabilised final structure was asymmetric (with the heights of the active and passive caps being different, as shown in Fig. 3i), as a consequence of the following two concomitant effects. First, the stiffness of the two membranes was different, due to a difference in the thickness of the adopted films (according to the values reported in the next section). Second, the Mullins effect [23] caused a stretch-induced softening of the passive membrane, due to the overstretch imposed during the depressurisation phase.

As the asymmetry of the device was expected to influence its performance, different prototypes with passive and active caps of different heights were assembled and compared. To this end, membranes made of three types of films having different initial thickness were used, evaluating four combinations, as described in the next section.

4.2 Comparisons among four sets of prototypes with different active cap height

From a geometrical standpoint, the conceived dynamic Braille dot can be regarded as the union of two ideally spherical caps, having the same base radius R but different heights h_a and h_p at electrical rest (no applied voltage), as represented in Fig. 4.

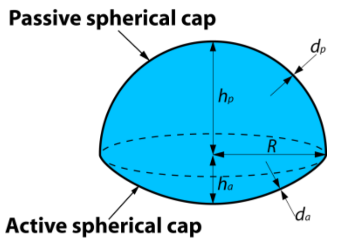

Fig. 4. Schematic geometrical representation of the proposed Braille dot.

The active and passive membranes have at electrical rest a thickness d_a and d_p, respectively.

In order to meet the geometrical Braille requirements, the dots were manufactured with a base radius R=750 μm and a passive cap height h_p of approximately 750 μm.

As the active cap height h_a was a free parameter for the actuator design, in this study its effect on the resulting performance was investigated by manufacturing four sets of different dots, made of different combinations of elastomers frequently employed for DE actuators in general. In particular, the four sets were obtained by using, as active and passive membranes, the following commercially available acrylic films by 3M: VHB 4910, VHB 4905 and VHB 9473PC. The tested combinations are presented in Table 2.

Table 2.

Combinations of elastomer films used to manufacture the active and passive membranes.

Actuator set	Active membrane	Passive membrane
1	VHB 4910	VHB 4905
2	VHB 4910	VHB 9473PC
3	VHB 4905	VHB 4905
4	VHB 4905	VHB 9473PC

During manufacturing, while the active cap height h_a was not controlled, the passive membrane was processed in such a way that the final passive cap height h_p was as close as possible to the targeted 750 µm for each set of prototypes. To this end, the applied depressurization (Fig. 3d) was empirically adjusted to a different level for each set. Adjustments were required, due to the different values of stiffness shown by the two membranes used in each set, as a consequence of their different thickness. Indeed, the thickness of the initial elastomer films in the non-stretched state was 1000, 500 and 250 µm, respectively for VHB 4910, 4905 and 9473PC, which then, upon the application of a 300% biaxial pre-strain, respectively reduced to about 62.5, 31.3 and 15.6 µm (calculated values). The thickness then further reduced as a result of the actuator assembly, owing to the hemispherical shaping of the membranes. The final values of the membrane thicknesses were computed as described in the next section.

4.3 Geometrical estimate of the thickness of the two membranes

A simple geometrical analysis of the structure allows for estimating d_a and d_p from measured values of h_a and h_p. Prior to providing the two membranes with a three-dimensional shape (while manufacturing the device), they initially consisted of flat circular elastomeric layers having a radius R and an initial thickness (immediately after the 300% biaxial prestretch) of $d_{a,0}$ and $d_{p,0}$, respectively. So, their initial surface S_0 and volumes $Vol_{a,0}$ and $Vol_{p,0}$ were:

$$S_0 = \pi R^2 \quad (2)$$

$$Vol_{a,0} = S_0 d_{a,0} \quad (3)$$

$$Vol_{p,0} = S_0 d_{p,0} \quad (4)$$

During the fabrication of the device, the active and passive membranes were deformed, such that their final shapes were ideally spherical caps, with surfaces S_a and S_p, respectively, given by the following expressions:

$$S_a = \pi\left(R^2 + {h_a}^2\right) \quad (5)$$

$$S_p = \pi\left(R^2 + {h_p}^2\right) \quad (6)$$

Furthermore, by considering that the thickness of the two membranes was negligible with respect to the cap height and base radius, the final volumes of the membranes Vol_a and Vol_p, respectively, could be approximated as follows:

$$Vol_a \cong S_a d_a \quad (7)$$

$$Vol_p \cong S_p d_p \quad (8)$$

Moreover, by assuming that each elastomeric membrane maintained a constant volume under deformation, the following can be seen:

$$S_0 d_{a,0} = S_a d_a \quad (9)$$

$$S_0 d_{p,0} = S_p d_p \quad (10)$$

Therefore, the final thickness of the membranes could be obtained as follows:

$$d_a \cong d_{a,0} \frac{R^2}{\left(R^2 + {h_a}^2\right)} \quad (11)$$

$$d_p \cong d_{p,0} \frac{R^2}{\left(R^2 + {h_p}^2\right)} \quad (12)$$

4.4 Measurement of the blocking force and stress relaxation

For each combination of active and passive membranes, three samples were manufactured and characterised in terms of blocking force and stress relaxation.

The blocking force was defined as the force generated by the Braille dot for a given applied displacement. It was measured with a double-column dynamometer (Z005, Zwick Roell, Germany), as follows. A cylindrical indenter, having a diameter of 2 mm, was connected to the machine’s load cell mounted on a mobile crossbar. The indenter was brought in contact with the Braille dot apex and the crossbar was displaced and maintained at a given position, so as to maintain the apex displaced, for 30 seconds, while the variation of force was recorded over time. The apex displacement corresponded to an indentation of the Braille dot. Measurements were taken for two values of indentation, 100 and 500 µm, as recommended in [1]. This procedure allowed for quantifying the force (and its relaxation over time) with which the Braille dot tends to resist the tactile action exerted by the user.

4.5 Measurement of the free stroke

Three samples for each combination of active and passive membranes were also characterised in terms of their free stroke, i.e. their voltage-induced displacement.

To this end, the displacement of the Braille dot apex, corresponding to an electrically generated reduction of the passive cap height, was measured using a laser-based displacement transducer (optoNCDT1800, Micro-Epsilon, Germany), according to general recommendations for free stroke measurements of DE actuators [24]. The free stroke was determined for step-wise voltages, whose amplitudes were varied with steps of 250 V, up to the actuator’s electrical breakdown (which changed according to the active membrane thickness). The corresponding maximum applied voltages (average values) for the actuator sets 1, 2, 3 and 4 (Table 2) were, respectively, 4.5, 4.5, 2.25 and 2.5 kV.

5. Results

5.1 Prototype samples of Braille dot

A prototype sample of the Braille dot is shown in Fig. 5.

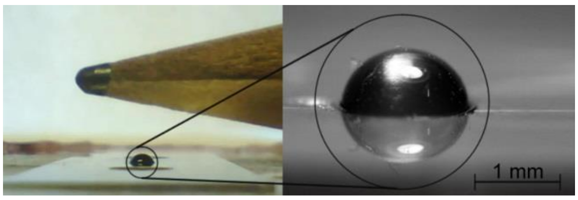

Fig. 5. Pictures of a prototype Braille dot at electrical rest.

Fig. 6 presents the measurements of the active and passive cap heights h_a and h_p at electrical rest (i.e. without any applied voltage) for the four sets of manufactured Braille dots.

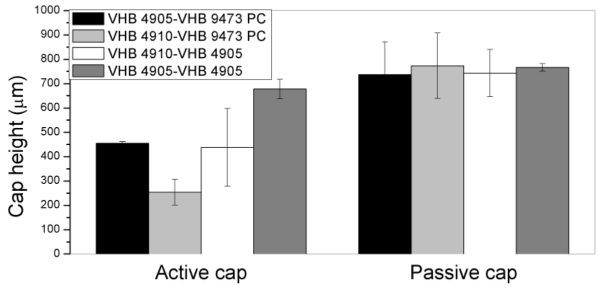

Fig. 6. Average active and passive cap heights h_a and h_p, at electrical rest, for the four sets of prototype Braille dots. Error bars represent the standard deviation related to the three samples tested for each set.

As shown by these data, the average passive cap height was about 750 μm for each set of prototypes, as intended. However, the active caps had a variable height, according to the differences in the stiffness of the membranes, due to the combination of different materials.

The average values of the cap heights were used to compute the average values of the thickness of the active and passive membranes, for each combination of materials, according to Eqs. (11) and (12). The computed values for the four sets of prototypes are presented in Table 3.

Table 3.

Average values at electrical rest of the thickness of the active and passive membranes.

		Active membrane	
		VHB 4910	VHB 4905
Passive membrane	VHB 4905	d_a=48.07 μm d_p=18.37 μm	d_a=18.2 μm d_p=16.31 μm
	VHB 9473 PC	d_a=56.6 μm d_p=8.14 μm	d_a=23.6 μm d_p=8.56 μm

5.2 Braille dot blocking force

Owing to the viscous nature of the elastomeric materials used to make the Braille dots, the four sets of prototype Braille dots were found to exhibit a significant stress relaxation. Fig. 7 presents results of a typical relaxation test.

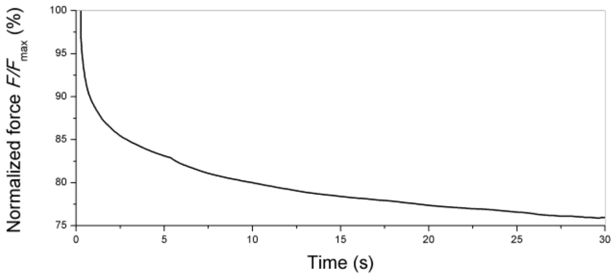

Fig. 7. Typical relaxation of the force generated by the Braille dot, for a given applied displacement.

In particular, the prototype dots exhibited a typical decrease in force of about 25% after 30 seconds.

Notwithstanding such a considerable drop of force over time, it is worth noting that the value at 30 seconds is not representative of the force that a user would actually experience while reading a Braille text. Indeed, Braille reading occurs via continuous movements of the finger over the dots, such that they are never solicited statically. The relevant variable is the time needed to slide the finger over a single dot, in order to estimate its height. This time can be evaluated as the mean time needed to read a letter (which for a Braille system is a group of eight dots), and it can be estimated as follows. Considering a reading rate of 100 words per minute [25] and an average of 5.1 letters per word in the English language [26], the resulting reading speed is 510 letters per minute, i.e. 8.5 letters per second. This implies that the user touches a new group of eight Braille dots approximately every 0.1 s. Therefore, it is important that the dot response in terms of force is guaranteed within about 0.1 s from the beginning of the contact with the finger.

So, the relevant values of force to be considered from the electromechanical characterisation are those measured at 0.1 s after the indentation onset. They are presented in Fig. 8, where they are also compared with the Braille requirements [1].

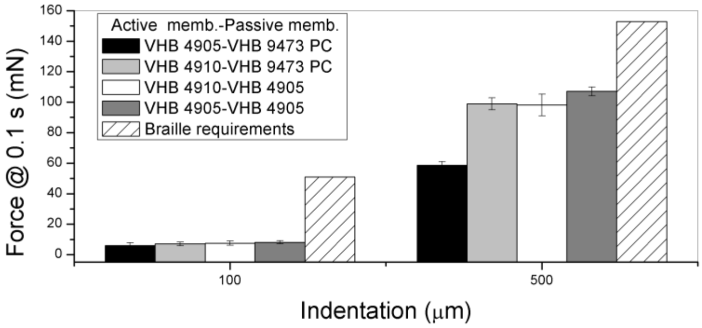

Fig. 8. Average blocking force at electrical rest, shown by each prototype Braille dot 0.1 s after its indentation. Values are reported for two levels of indentation. Error bars represent the standard deviation related to the three samples tested for each set of prototypes.

5.3 Voltage-induced Braille dot displacement

An electrically induced displacement of a prototype Braille dot is shown in Fig. 9.

Fig. 9. Picture of a prototype Braille dot at rest (left) and when a voltage is applied (right). A video of the dot in action is available at https://www.youtube.com/watch?v=8mSCbKlTcO0.

The typical response time to reach 90% of the final dot height was about 2 s.

Fig. 10 presents, for each set of prototypes, the steady-state electrically-induced displacement of the Braille dot apex, as a function of the voltage normalised by the active membrane thickness at electrical rest d_a.

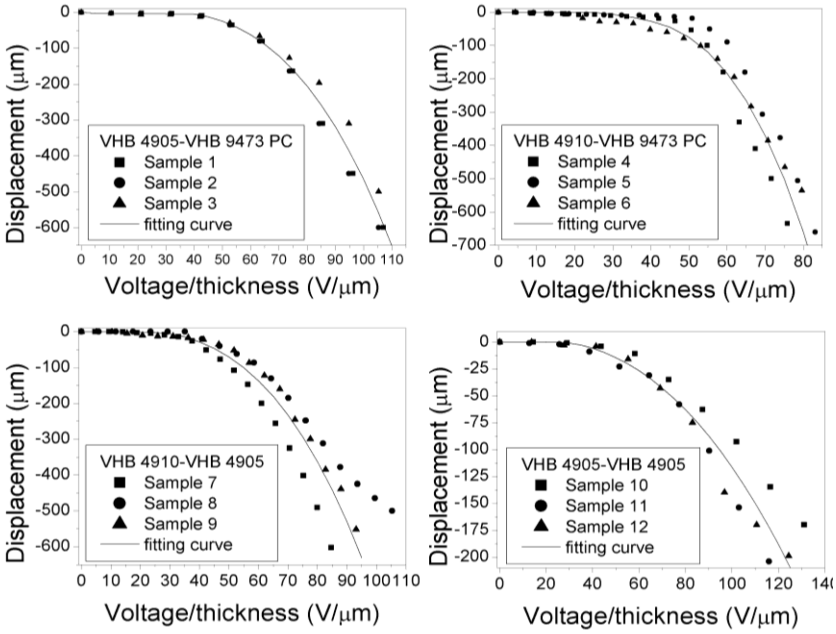

Fig. 10. Voltage-induced displacement of the Braille dot apex for the four sets of prototype dots. A data fitting line for each set is used as a guide for the eye.

For the sake of a direct comparison of the performance shown by the four sets of prototype dots, Fig. 11 presents a co-plot of the fitting lines extracted from Fig. 1010.

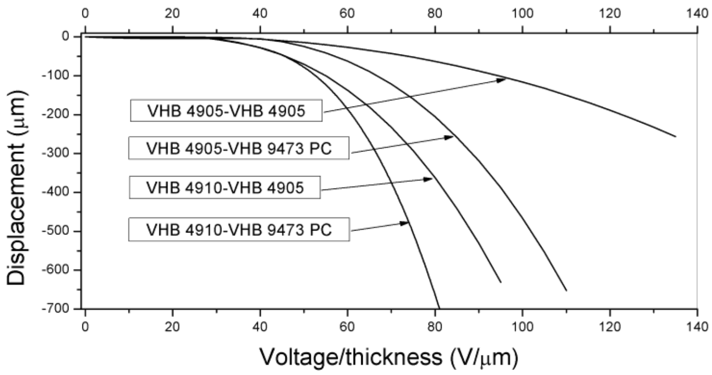

Fig. 11. Comparison of the actuation performance of the four sets of prototype Braille dots.

The effect of the active cap height at electrical rest h_a on the achievable displacement is presented in Fig. 12, which plots the displacement at 75 V/μm (arbitrarily chosen as a reference value from Fig. 11), as a function of the cap height for each sample of each set of Braille dots.

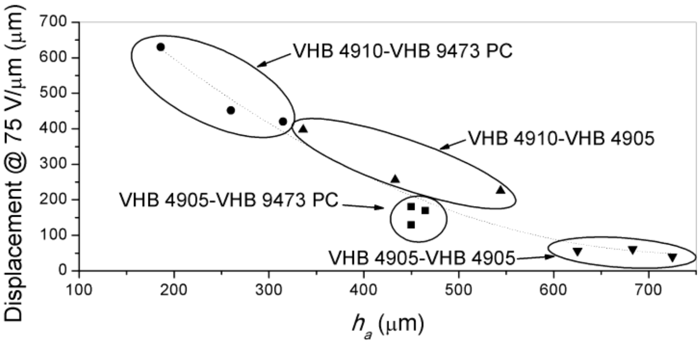

Fig. 12. Braille dot apex displacement obtained at 75 V/μm as a function of the active cap height at electrical rest, for each prototype Braille dot.

The average value of the displacements at 75 V/μm is shown, for each set of prototypes, in Fig. 13, which also displays the related asymmetry of the dots in the active and passive states.

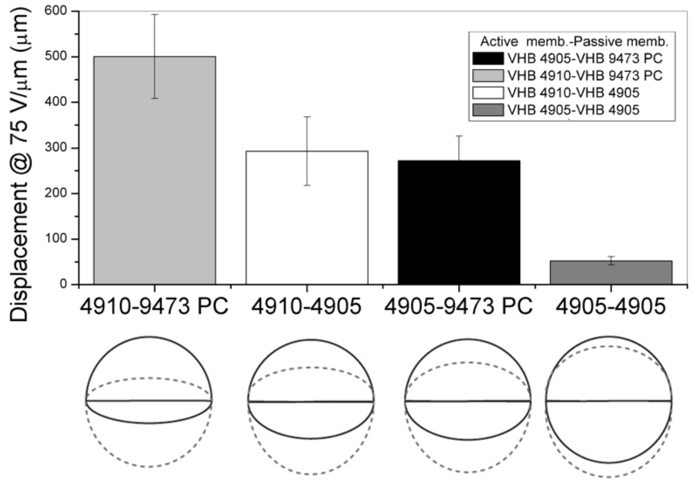

Fig. 13. Average displacement at 75 V/μm for the four sets of prototype Braille dot. Error bars represent the standard deviation related to the three samples tested for each set. The schematic drawing associated to each set represents, qualitatively, a cross-section of the asymmetric dot in the passive state (solid line) and active state (dotted line).

6. Discussion

6.1 Compact size enabling multiple-line portable displays

As compared to commercial systems, the design proposed here has the unique advantage of fusing in the same structure the Braille dot and its driving mechanism.

The consequent significant reduction of the lateral size of the actuation part makes the proposed solution suitable to the creation of an array of multiple dots in multiple lines, as required by the development of full-page Braille displays. Furthermore, the significant reduction also of the vertical size makes the design potentially suitable to obtain thin and lightweight displays, thus enabling portability, possibly also creating hand-held devices.

6.2 Achievable blocking force

Fig. 8 shows that, in order to comply with Braille requirements in terms of blocking force, further improvements are necessary. Indeed, although for some Braille readers with light touch the force generated by these prototypes might be sufficient, for others it may result in a so-called tactile noise [1]. Increasing the dot's passive (i.e. elastic or, better, hyperelastic) force requires a stiffening of the membranes.

This could be obtained in different ways. While using stiffer elastomers and/or thicker passive membranes would be a simple approach, it is not advisable as it would reduce the achievable active displacements. Moreover, if applied to the active membrane, it would also increase the required driving voltage. To avoid these drawbacks, a more promising, although even more challenging, strategy is to create a multi-layered active membrane, by stacking multiple dielectric films intertwined to multiple compliant electrodes. This would increase the active membrane total thickness, while preserving a low separation between the electrode pairs so as not to increase the required driving voltage.

6.3 Achievable displacement

As expected, the asymmetry of the Braille dot influenced its performance in terms of achievable displacement (Fig. 13). In particular, the average displacement at 75 V/μm was about 500 μm for the set

VHB 4910-VHB 9473PC, which had the lowest height of the active cap at rest. The dots with increasing values of that height showed decreasing displacement.

This evidence could be interpreted by assuming that the flatter active caps corresponded to less stretched active membranes, which were therefore less stiff (it is worth noting that during manufacturing each membrane was bi-axially pre-stretched above the flex point of its stress-strain curve). The lower stiffness determined a higher active deformation in response to any given electrical stimulus.

It is worth noting that the softest set of dots did not show the highest deformation. Indeed, the stiffness inferable from data reported in Fig. 8 is not representative of the stiffness of the active membrane only.

6.4 Selection of the best trade-off configuration

The set of prototypes VHB 4910-VHB 9473PC offered the best trade off in terms of performance. Indeed, as shown in Figs. 8 and 12, it allowed for a maximisation of the displacement while providing a force just 10% smaller than the maximum value recorded.

6.5 High voltage driving

One of the major drawbacks of the proposed technology is represented by the need for high driving voltages. This introduces a limitation in terms of size, safety and cost of the required electronics, as discussed below.

The generation of voltages as high as those used in this work is *per se* not particularly problematic from a technical standpoint or particularly dangerous in terms of electrical safety, considering that there is no need for high driving powers (the loads are capacitive) and that all the high-voltage parts are insulated. Indeed, the generation of voltages of the order of 1 kV has been demonstrated for micro-battery powered systems using compact voltage multipliers, as discussed in [27], enabling the development of single-channel systems that are both portable and relatively safe.

However, the electrical driving of arrays of multiple actuators is more challenging, as it implies the control of several high-voltage channels. The most straightforward approach that could be considered requires the use of one high voltage converter for each actuator, but this would excessively increase the size, cost and power consumption of the system. Overcoming this problem requires the adoption of driving strategies specifically designed for this application. An example could consist in multiplexing a single high-voltage source (for example by using high voltage MOSFETs) while using the control strategy called Dynamic Scanning Actuation proposed by Koo et al. [28]. With that strategy, one line of the array delivers the high voltage, while a second line is grounded. Actuation is triggered only when both the lines are active, so that, by sequentially scanning each line, it is possible to continuously refresh each actuator's state, setting it to the desired value (on or off).

Notwithstanding such approaches for the driving electronics, the major drawbacks are still represented by its size and cost, since, as compared to low-voltage units, high-voltage components are more difficult to miniaturise and have relatively lower market share. So, the reduction of the driving voltage is imperative in order to unleash the real potential of the DE actuation technology for Braille displays.

To this end, future developments should be aimed at lowering the voltages down to about 200 V, which is the standard for the low-cost and low-size drives of piezoelectric transducers (available in a huge diversity of products today). To address this need, according to Eq. (1) there are two strategies: i) synthesis of new elastomers with higher dielectric constant [29, 30]; ii) processing the elastomers as thinner films. Reaching these targets requires the use of silicone elastomers, as in general they combine ease of material processing with very low viscosity that enables a higher actuation speed [31]. Custom manufacturing processes are necessary to reduce the thickness ideally down to a few microns. Although this is challenging for highly stretchable materials, preliminary evidences indicate feasibility [32]. On the other hand, in order to avoid a reduction of the elastic force due to the reduction of the active membrane thickness, it will be necessary to create a multi-layer structure, as discussed previously.

6.6 Other uses of the proposed new technology

The actuation technology presented here might be considered also for other types of tactile displays, not necessarily intended for the blind people. For instance, arrays of tactile elements might be integrated within user interfaces and control panels, to enable tactile feedback aimed at enhancing human-machine interactions.

7. Conclusions

In this work we presented a concept to enable the development of dynamic Braille dots for multiple-lines refreshable Braille displays that can be portable and affordable. Prototype samples of these new refreshable Braille dots were assembled using off-the-shelf materials and adopting tools and procedures not yet optimised. Whereas the prototypes allowed for a proof-of-concept demonstration of the functionality of the proposed concept, they also showed the required future improvements. These include the need for processing more suitable elastomers as thinner films and using them to assemble multi-layer structures, which should be extensively characterised also in terms of cycle lifetime. Overall, these suggested developments define a road map towards the first Braille tablets.

Competing interests

None declared

Funding

None

Ethical approval

Not required

References

[1] N. H. Runyan, and F. Carpi, “Seeking the 'holy Braille' display: might electromechanically active polymers be the solution?,” Expert Review of Medical Devices, vol. 8, no. 5, pp. 529-532, 2011.

[2] D. Kendrick, “Freedom Scientific Focusing On Braille Part 2: A Review of the Focus Blue 40 Braille Display,” American Foundation for the Blind Magazine, vol. 15, no. 9, pp. 2-3, 2014.

[3] HyperBraille; [Online]. Available: http://web.metec-ag.de/graphik display.html.

[4] National Federation of the Blind, “The braille literacy crisis in America: Facing the truth, reversing the trend, empowering the blind”; [Online]. Available: http://www.nfb.org.

[5] L. Yobas, D. M. Durand, G. G. Skebe, F. J. Lisy, and M. Huff, “A novel integrable microvalve for refreshable Braille display system,” Journal of Microelectromechanical Systems, vol. 12, no. 3, pp. 252-263, 2003.

[6] Y. Haga, W. Makishi, K. Iwami, K. Totsu, K. Nakamura, and M. Esashi, “Dynamic Braille display using SMA coil actuator and magnetic latch,” Sensors and Actuators A: Physical, vol. 119, no. 2, pp. 316-322, 2005.

[7] K. Ren, S. Liu, M. Lin, Y. Wang, and Q. Zhang, “A compact electroactive polymer actuator suitable for refreshable Braille display,” Sensors and Actuators A: Physical, vol. 143, no. 2, pp. 335-342, 2008.

[8] P. Chakraborti, H. K. Toprakci, P. Yang, N. Di Spigna, P. Franzon, and T. Ghosh, “A compact dielectric elastomer tubular actuator for refreshable Braille displays,” Sensors and Actuators A: Physical, vol. 179, pp. 151-157, 2012.

[9] P. Brochu, and Q. Pei, “Advances in dielectric elastomers for actuators and artificial muscles,” Macromolecular Rapid Communications, vol. 31, no. 1, pp. 10-36, 2010.

[10] F. Carpi, D. De Rossi, R. Kornbluh, R. E. Pelrine, and P. Sommer-Larsen, Dielectric Elastomers as Electromechanical Eransducers: Fundamentals, Materials, Devices, Models and Applications of an Emerging Electroactive Polymer Technology, Oxford: Elsevier, 2008.

[11] R. Pelrine, R. Kornbluh, Q. Pei, and J. Joseph, “High-speed electrically actuated elastomers with strain greater than 100%,” Science, vol. 287, no. 5454, pp. 836-839, 2000.

[12] F. Carpi, Electromechanically Active Polymers: A Concise Reference, Zurich: Springer International Publishing, 2016.

[13] F. Carpi, and E. Smela, Biomedical Applications of Electroactive Polymer Actuators, Chichester: John Wiley & Sons, 2009.

[14] F. Carpi, S. Bauer, and D. De Rossi, “Stretching dielectric elastomer performance,” Science, vol. 330, no. 6012, pp. 1759-1761, 2010.

[15] N. Di Spigna, P. Chakraborti, D. Winick, P. Yang, T. Ghosh, and P. Franzon, “The integration of novel EAP-based Braille cells for use in a refreshable tactile display,” in Proc. of SPIE, Vol., 7642, 2010, pp. 76420A-76420A-9.

[16] R. Heydt, and S. Chhokar, “Refreshable Braille display based on electroactive polymers,” in Proc. 23rd Intl. Display Res. Conf., Phoenix, Arizona, 15–18 September, 2003, pp. 5.

[17] H. R. Choi, I. M. Koo, K. Jung, S.-g. Roh, J. C. Koo, J. Nam, and Y. K. Lee, "A Braille display system for the visually disabled using a polymer based soft actuator," In Biomedical Applications of Electroactive Polymer Actuators, F. Carpi, and E. Smela, Editors, pp. 427-442, Chichester: Wiley, 2009.

[18] H. S. Lee, H. Phung, D.-H. Lee, U. K. Kim, C. T. Nguyen, H. Moon, J. C. Koo, and H. R. Choi, "Design analysis and fabrication of arrayed tactile display based on dielectric elastomer actuator," Sensors and Actuators A: Physical, vol. 205, pp. 191-198, 2014.

[19] M. Matysek, P. Lotz, and H. F. Schlaak, "Tactile display with dielectric multilayer elastomer actuators," in Proc. of SPIE, Vol. 7287, 2009, pp. 72871D-72871D-9.

[20] Z. Yu, W. Yuan, P. Brochu, B. Chen, Z. Liu, and Q. Pei, "Large-strain, rigid-to-rigid deformation of bistable electroactive polymers," Applied Physics Letters, vol. 95, no. 19, pp. 192904, 2009.

[21] F. Carpi, G. Frediani, and D. De-Rossi, "Hydrostatically coupled dielectric elastomer actuators," IEEE/ASME Transactions on Mechatronics, vol. 15, no. 2, pp. 308-315, 2010.

[22] S. J. A. Koh, T. Li, J. Zhou, X. Zhao, W. Hong, J. Zhu, and Z. Suo, "Mechanisms of large actuation strain in dielectric elastomers," Journal of Polymer Science Part B: Polymer Physics, vol. 49, no. 7, pp. 504-515, 2011.

[23] L. Mullins, "Softening of rubber by deformation," Rubber Chemistry and Technology, vol. 42, no. 1, pp. 339-362, 1969.

[24] F. Carpi, I. Anderson, S. Bauer, G. Frediani, G. Gallone, M. Gei, C. Graaf, C. Jean-Mistral, W. Kaal, G. Kofod, M. Kollosche, R. Kornbluh, B. Lassen, M. Matysek, S. Michel, S. Nowak, B. O'Brien, Q. Pei, R. Pelrine, B. Rechenbach, S. Rosset, and H. Shea, "Standards for dielectric elastomer transducers," Smart Materials and Structures, vol. 24, no. 10, pp. 105025-1 – 105025-25, 2015.

[25] P. Mousty, and P. Bertelson, "A study of braille reading: 1. Reading speed as a function of hand usage and context," The Quarterly Journal of Experimental Psychology, vol. 37, no. 2, pp. 217-233, 1985.

[26] Web search: "Average word length in the English language"; [Online]. Available: http://www.wolframalpha.com/input/?i=average+word+length+English+language.

[27] G. Frediani, D. Mazzei, D. De Rossi, and F. Carpi, "Wearable wireless tactile display for virtual interactions with soft bodies," Frontiers in Bioengineering and Biotechnology, vol. 2, Article 31, pp. 1-7, 2014.

[28] I. Koo, K. Jung, J. Koo, J. D. Nam, Y. Lee, and H. R. Choi, "Wearable fingertip tactile display," in Proc. of 2006 Sice-Icase International Joint Conference, Busan, 2006, pp. 1911-1916.

[29] F. B. Madsen, A. E. Daugaard, S. Hvilsted, and A. L. Skov, "The Current State of Silicone-Based Dielectric Elastomer Transducers," Macromolecular Rapid Communications, vol. 37, no. 5, pp. 378-413, 2016.

[30] S. J. Dünki, Y. S. Ko, F. A. Nüesch, and D. M. Opris, "Self-Repairable, High Permittivity Dielectric Elastomers with Large Actuation Strains at Low Electric Fields," Advanced Functional Materials, vol. 25, no. 16, pp. 2467-2475, 2015.

[31] L. Maffli, S. Rosset, M. Ghilardi, F. Carpi, and H. Shea, "Ultrafast All-Polymer Electrically Tunable Silicone Lenses," Advanced Functional Materials, vol. 25, no. 11, pp. 1656-1665, 2015.

[32] A. Poulin, S. Rosset, and H. R. Shea, "Printing low-voltage dielectric elastomer actuators," Applied Physics Letters, vol. 107, no. 24, pp. 244104, 2015.